

Asymmetric space-dependent systems: Partial stabilization through the addition of noise and exact solutions for the corresponding nonlinear Langevin equations

Kwok Sau Fa * ^{†,1}, Choon-Lin Ho,² Y. B. Matos,¹ and M. G. E. da Luz ^{‡1}

¹*Departamento de Física, Universidade Federal do Paraná, 81531-980 Curitiba-PR, Brazil*

²*Department of Physics, Tamkang University, Tamsui 25137, Taiwan*

Abstract

In many instances, the dynamical richness and complexity observed in natural phenomena can be related to stochastic drives influencing their temporal evolution. For example, random noise allied to spatial asymmetries may induce stabilization of otherwise diverging trajectories in dynamical systems. However, to identify how exactly this takes place in actual processes usually is not a simple task. Here we unveil a few trends leading to dynamical stabilization and diversity of behavior by introducing Gaussian white noise to a class of exactly solvable non-linear deterministic models displaying space-dependent drifts. For the resulting nonlinear Langevin equations, the associated Fokker-Planck equations can be solved through the similarity method or the Fourier transform technique. By comparing the cases with and without noise, we discuss the changes in the systems dynamical characteristics. Simple examples of drift and diffusion coefficients are explicitly analyzed and comparisons with some other models in the literature are made. Our study illustrates the rich phenomenology originated from spatially heterogeneous dynamical systems under the influence of white noise.

* Permanent address: Department of Physics, Universidade Estadual de Maringá, Av. Colombo 5790, 87020-900, Maringá-PR, Brazil

[†] corresponding author email: kwok@dfi.uem.br

[‡] email: luz@fisica.ufpr.br

I. INTRODUCTION

The great assortment of responses to external stimuli is one of the key factors generating the behavioral diversity common to many natural phenomena [1, 2]. For instance, this can give rise to the emergence of complexity and spatial-temporal patterns in a broad range of processes [3, 4], even if they are restricted to certain constraints (say, having to follow a gradient flow) as in the evolution of coarsening systems [5, 6].

There are distinct features allowing for such variety of evolution trends (for a review see, e.g., [7]). But certainly, spatial heterogeneities and/or asymmetries are among the most ubiquitous ones [8–11]. Actually, effects like spatial-temporal oscillations [12], resonances [13] and strong dispersion [14] can all be triggered by inhomogeneous environments. This is particularly true in biologically-related problems where space-dependent coefficients may greatly influence the variability of population genetics [15–17] and growth [18–25], the type of diffusion across membranes [26], and the onset of anomalous mobility [27], just to cite a few examples. It is also needless to emphasize that landscape profile changes are fundamental to understand large and strongly correlated systems, as in ecology [4, 9, 10].

Nonetheless, as relevant as to induce distinct compartment, spatially asymmetric interactions and drives have a crucial role in stabilizing, synchronizing and promoting cooperative feedback [28–32]. On the one hand, these characteristics are essential to maintain the functional diversity in the natural world [33–37], preventing trivial dynamics [7]. On the other hand, the existence of a phase or state space displaying multi-stability [38, 39] (conceivably created by heterogeneous media) is not enough to avoid trivial (stable) attractors [40]. Thence, escaping or switching mechanisms from dynamical traps [41, 42] are commonly found in systems presenting diversity of behavior, notably in non-equilibrium as well as in complex systems [43]. Given that randomness is rather effective in generating such types of mechanisms [44, 45], the somewhat omnipresence of stochasticity in a huge number of physical phenomena is far from being a surprise [1, 2, 36, 45].

The above discussion supports the recognized significance of the generalized Langevin equation (GLE) in describing countless realistic processes, appealing rather directly to our intuition (for an overview see [46] as well the refs. therein). Broadly, it combines the deterministic Newton’s second law with external stochastic forces [47–54]. However, the GLE is a stochastic differential equation, often being difficult to treat for arbitrary drifts

and random forces. One possible approach is then to convert the GLE into the Fokker-Planck equation, determining an associated probability density function (PDF) for relevant quantities [47, 55–58]. In this way, one can exploit a large number of methods available in the literature for solving differential equations. This constitutes a traditional framework to tackle innumerable problems, particularly those whose physical parameters depend non-trivially on space. As illustrations we mention the modeling of: transport processes [59, 60], organic semiconductors [61], star-shaped polymer translocation into a nanochannel [62], periodic porous material [63], and turbulent two-particle diffusion in configuration space [64–68]. Further, in the case of drifts with time-dependent coefficients (even if implicitly), the Fokker-Planck equation approach helps to understand unusual dynamics, as the asymptotic of continuous time random walk models [69–71], logarithmic oscillations for moments of physical variables [72] and dynamical diversity for systems driven by colored noise [73–82].

In this contribution we shall address the interplay between deterministic and stochastic drives in establishing time evolution traits. We discuss a way to avoid (1) steadily stopping and (2) monotonic diverging orbits by adding noise to a class of spatially asymmetric problems, partially stabilizing the systems [38] and thus allowing richer dynamics [1, 2, 7]. We note there is a vast literature rigorously classifying richness (i.e., diversity of behavior) in dynamical systems, see e.g. [83]. Here we assume a straightforward point of view. So, by richer we just means to have arbitrary (eventually involved and irregular [83, 84]) trajectories, but precluding the above asymptotic tendencies (1) and (2).

To keep the problem as simple as possible, although displaying spatial heterogeneity, we suppose a set of one-dimensional first-order differential equations, whose drift coefficients depend on the sign of their dependent variable $x(t)$ (see next Section). Given their functional form $dx(t)/dt = F(x; \Lambda)$ — with Λ representing the collection of parameters — straightforward dynamics is simple to identify. Indeed, they correspond to $dx(t)/dt = 0$ for some finite time $t = \tau$, case (1), or $dx(t)/dt > 0$ ($dx(t)/dt < 0$) for all t , case (2). For our prototype models we first show that the pure deterministic evolution tends to be rather trivial in the aforementioned sense for a very large region of the Λ space. Then, we include into the equations a generic multiplicative noise term driven by Gaussian white noise under the Stratonovich prescription. This yields nonlinear Langevin equations, displaying anomalous diffusion.

Following a previously developed method [85] and a transformation scheme amenable

to problems possessing scaling similarity [52, 86–90], we are able to exactly solve the related Fokker-Planck equation for a considerably large range of parameter values. For some instances where such prescription does not work, we use the Fourier transform technique. From the analytic solutions we analyze the difference between the evolution with and without the stochastic component. In particular, we examine how the stochasticity evades dynamical steady behavior, partially stabilizing the systems, and also how the emerging evolution diversity depends on the specific regions of the Λ space.

Finally, concrete simple examples are explored in more details. The resulting PDFs are studied for some parameter values and a few cases are compared with related traditional models in the literature.

II. THE SET OF MODELS

As stated in the introduction section, our goal is to unveil potential mechanisms (based on the addition of noise) preventing the systems to go into trivial time evolutions, as the previously mentioned instances (1) and (2). So, we shall work directly with the systems velocity dx/dt and thus to consider first-order differential equations, relevant in distinct problems where the interest relies on the configuration space dynamics [91]. We emphasize that our focus here is not in any specific physical system. Therefore, our choice of F in $dx(t)/dt = F(x; \Lambda)$ below is such that it: does present asymmetric spatial dependence, in certain conditions can give rise to dynamical richness, is amenable to analytic solutions and finally, for certain values of the parameters recovers known models in the literature.

A. Deterministic dynamical system

Consider a one-dimensional dynamical variable $x(t)$, whose evolution is governed by the equation

$$\frac{dx(t)}{dt} = F(x; \Lambda = \{a, b, \mu\}) = \left(a - b \mu \frac{\text{sign}(G(x))}{2} \right) |G(x)|^{\mu-1} D(x), \quad (1)$$

with initial condition $x(t_0) = x_0$. Here, a , b and μ are real numbers with $b > 0$, $\text{sign}[\cdot]$ is the sign function, $D(x)$ is a given everywhere non-negative function of x , and $G(x)$ relates

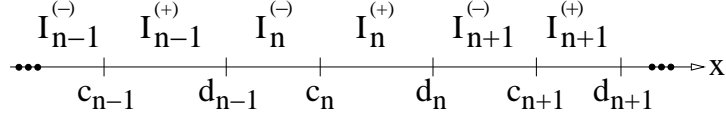


FIG. 1: Schematics of the successive distinct intervals along x for which the function $G(x)$, basically the integral of $D(x)$, changes its sign.

to $D(x)$ through

$$\frac{dG(x)}{dx} = \frac{1}{D(x)}. \quad (2)$$

Different $D(x)$'s specify distinct drift terms and so we have in fact a set of systems. Moreover, as we are going to see along this work, the present functional form for our first order differential equation comply with all the desired features listed in the beginning of the section.

Although $D(x) \geq 0$, $G(x)$ may assume positive or negative values depending on x . Thus, along the infinite line x we can identify the intervals $c_n < x < d_n$ as $I_n^{(+)}$ and $d_{n-1} < x < c_n$ as $I_n^{(-)}$ (see Fig. 1), such that in $I_n^{(+)}$ ($I_n^{(-)}$) the function $G(x) > 0$ ($G(x) < 0$). By supposing $G(x)$ a continuous function, for any integer $n \in (N_l, N_r)$, inevitably $G(c_n) = G(d_n) = 0$. This is not the case if we allow “jumps” for $G(x)$ whenever x crosses over between positive and negative intervals $I^{(+)}$ and $I^{(-)}$. If for all $x > x_r$ ($x < x_l$), $\text{sign}(G(x))$ does not change, then N_r (N_l) is a finite integer, otherwise $N_r \rightarrow \infty$ ($N_l \rightarrow -\infty$).

By noticing that $|G(x)|^{\mu-1}D(x)$ is never negative, in principle the term $\text{sign}[G(x)]$ in Eq. (1) should give rise to a non-trivial spatially asymmetric evolution depending on the parameter values. To see why, let us consider that during the time interval $\mathcal{I}_T : t_0 \leq t < T$, the r-h-s of Eq. (1) does not vanish. Hence

- (i) For $|a|/b > |\mu|/2$ the time derivative of x has always the same sign of a . As a consequence, $x(t)$ presents a steady increasing ($a > 0$) or decreasing ($a < 0$) behavior for $t \in \mathcal{I}_T$ regardless of the functional form of $G(x)$.
- (ii) On the other hand, for $|\mu|/2 > |a|/b$, it follows that $dx(t)/dt$ has the same sign of $-\mu G(x)$. Therefore, along the evolution of $x(t)$ in the time interval \mathcal{I}_T , we have a switching in the variation of $x(t)$ whenever $G(x(t))$ reverses its sign, conceivably originating a rich dynamics depending on $D(x)$.

However, the system ceases to evolve when the r-h-s of Eq. (1) becomes zero. This

always takes place if along the time evolution of $x(t)$ there is a $x(\bar{t}) = \bar{x}$ such that either $a/b - \text{sign}[G(\bar{x})] \mu/2 = 0$ (in which case $|a|/b = |\mu|/2$) or

$$|G(\bar{x})|^{\mu-1} D(\bar{x}) = 0. \quad (3)$$

Disregarding the too specific and trivial situation of $|a|/b = |\mu|/2$, for an oscillatory-like dynamics described in (ii) to occur (say, within the interval (x_{min}, x_{max})), Eq. (3) must be precluded. For so, we observe that if $D(\bar{x}) = 0$ ($|G(\bar{x})|^{\mu-1} = 0$) then $|G(\bar{x})|^{\mu-1} (D(\bar{x}))$ must diverge in such a way to maintain their product non-null as $x \rightarrow \bar{x}$. Therefore, we suppose that in the vicinity of \bar{x} the leading term from either a Taylor or a Laurent series for $D(x)$ and $G(x)$ is (for both $\nu, \gamma \neq 0$)

$$D(x) \approx d(x - \bar{x})^\nu, \quad G(x) \approx g(x - \bar{x})^\gamma, \quad (4)$$

with the constants $d, g \neq 0$. So, we should have

$$\nu + (\mu - 1) \gamma \leq 0 \quad \Rightarrow \quad \nu \leq (1 - \mu) \gamma. \quad (5)$$

Moreover, from Eqs. (2) and (4) it follows that $gd\gamma \approx 1$ and $\gamma + \nu \approx 1$, thus

$$(2 - \mu) \nu \leq 1 - \mu. \quad (6)$$

We remark that Eq. (6) fails when $\mu = 2$.

Particular cases are easily derived from the above. Let us assume \bar{x} in the interval of interest (x_{min}, x_{max}) , then Eq. (3) is not verified at $x = \bar{x}$ in the following situations:

- (a) If $\mu = 1$, when $D(\bar{x}) \neq 0$. Thence, in the full x interval we must have $D(x) > 0$.
- (b) For $D(\bar{x}) = 0$ (so $\nu > 0$) then: (b-1) if $\mu < 1$, when $\nu \leq (1 - \mu)/(2 - \mu) < 1$ (so that $G(\bar{x}) = 0$); (b-2) if $\mu > 2$, when $\nu \geq (\mu - 1)/(\mu - 2) > 1$ (such that $G(\bar{x})$ diverges).
- (c) For $\mu > 1$ and $G(\bar{x}) = 0$, when $1 < \mu < 2$. In fact, here we must have a diverging $D(\bar{x})$, implying in $\nu < 0$. This condition requires the mentioned range for μ .
- (d) If there are jumps in $D(x)$, so that $G(x)$ can change sign but without passing through zero, then when $D(x) > 0$. However, in such case we should define a proper prescription for Eq. (2) at these discontinuities.

It is clear from the above analysis that only for specifically chosen functions $D(x)$ and parameter values, namely, those observing the restrictions (a)–(d), the asymmetric term in Eq. (1) can yield a more diverse, eventually stable or limited in space, dynamics. This is in opposition to a simple, as sink or diverging, basins of attraction emerging from Eq. (1) for generic $D(x)$'s, i.e., functions not complying with (a)–(d).

We now illustrate the previous discussion with three examples of $D(x)$ and the associated $G(x)$ in Fig. 2, assuming the parameters in the range specified by (ii). In order to observe the condition (d), we have functions with proper jumps shown in Fig. 2 (a). In this case $|G(x)|^{\mu-1} D(x)$ is never null, but at the expense of rather specially tailored discontinuous $D(x)$ and $G(x)$. In Fig. 2 (b), $D(x) = \sin^2[x]$ and $G(x) = -\cot[x]$, with $\mu = 3$. At the zeros of $D(x)$, one finds that $G(x)^2 D(x) > 0$, hence precluding Eq. (3), since the condition (b) is verified (note that $G(x)$ diverges at these points). Nevertheless, at the zeros of $G(x)$ we can not also avoid $G(x)^2 D(x)$ to vanish, so with Eq. (3) holding true. Consequently, the system dynamics necessarily halts at these sink points. Lastly, for $D(x) = 1/2 + \sin^2[x]$, $G(x) = 2 \operatorname{artan}[\sqrt{3} \tan[x]]/\sqrt{3}$ and $\mu = 11/10$, we have that $|G(x)|^{0.1} D(x)$ is never null. But this demands very narrow divergences for $|G(x)|^{0.1} D(x)$ (observe the spikes in the Fig. 2 (c)), hence also for $dx(t)/dt$, whenever x is very close to multiples of π . This type of drift might be unacceptable in modeling distinct processes.

In this way, a natural question is: What would stabilize our family of dynamical systems, averting a trivial evolution from Eq. (1) (where by trivial we mean $x(t)$ either becoming stationary or monotonically evolving towards $\pm\infty$) for a much broader set of functions $D(x)$ and parameter values? We shall demonstrate below this can be achieved via stochastic noise added to the original deterministic problem.

For completeness, the formal general solution of the present dynamical system in each interval $I^{(\pm)}$ is presented in the A.

B. Adding stochastic noise

Hereafter we consider a noise term in our original family of systems. In doing so, we obtain a nonlinear Langevin equation with space-dependent drift and diffusion coefficients

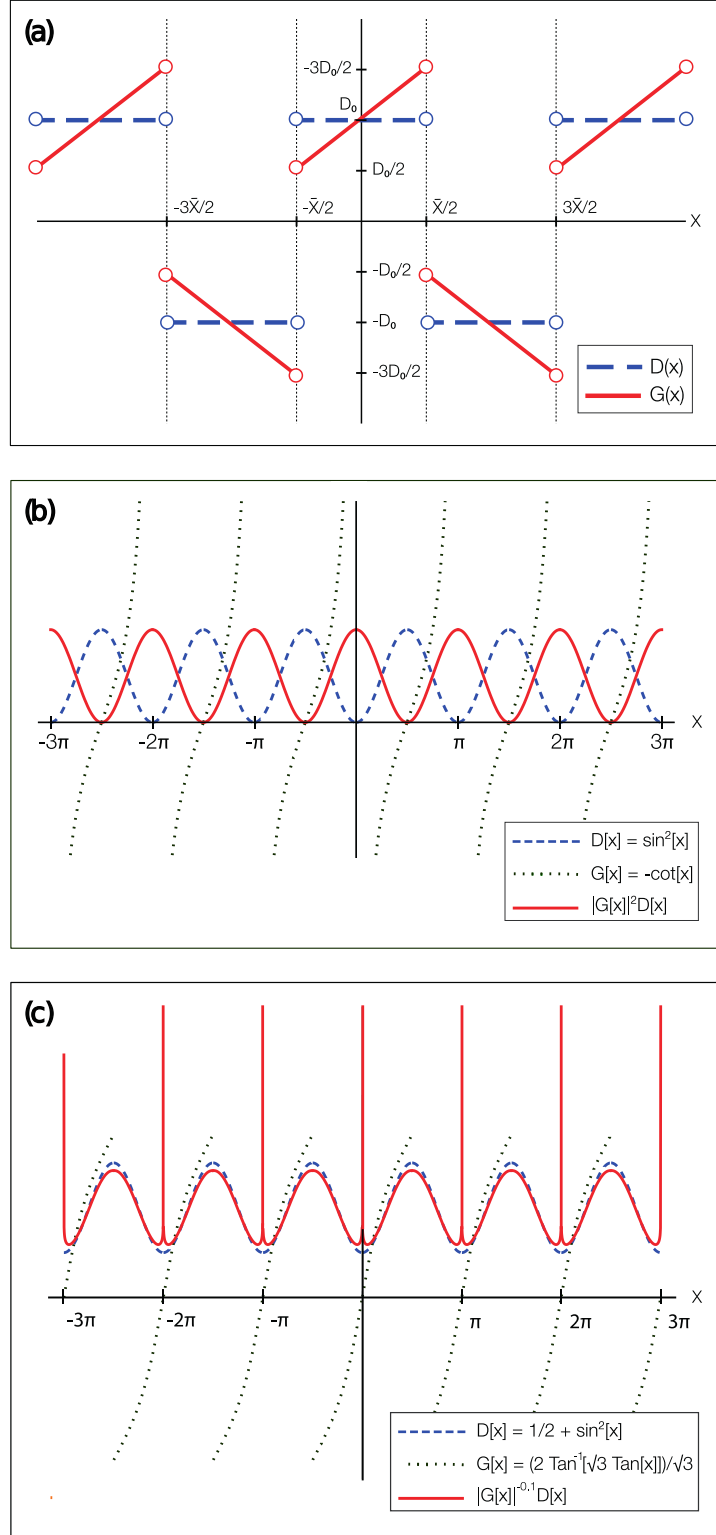


FIG. 2: Three examples of $D(x)$ and $G(x)$. In (a) and (c), the term $|G(x)|^{\mu-1} D(x)$ is never zero, potentially resulting in a rich dynamics for $x(t)$. But this requires very particular and singular functions. In (b) although $|G(x)|^{\mu-1} D(x)$ does not vanish at the points where $D(x) = 0$, this cannot be avoided for the points where $G(x) = 0$, eventually driving the system to a stationary behavior.

and driven by the Gaussian white noise (in the Stratonovich description), or

$$\frac{dx(t)}{dt} = \left(a - b\mu \frac{\text{sign}(G(x))}{2} \right) |G(x)|^{\mu-1} D(x) + \sqrt{b} |G(x)|^{\mu/2} D(x) L(t). \quad (7)$$

The parameter ranges and relation between $D(x)$ and $G(x)$ are as before. The white noise force, $L(t)$, is such that [47]

$$\langle L(t) \rangle = 0, \quad \langle L(t)L(t') \rangle = 2\delta(t-t'), \quad (8)$$

where $\delta(t)$ is the Dirac delta function.

Now we should emphasize that the previous situation of dynamical traps for the deterministic model, represented by Eq. (3), is far less common here. Indeed, provided $a \pm b\mu/2 \neq 0$ and $\mu \neq 2$ in Eq. (7), for a given $x(t) = \bar{x}$ to lead to $dx(t)/dt = 0$ (so stationary) independently on the noise $L(t)$, it should, at once, satisfy Eq. (3) as well as an akin relation with $\mu - 1 \rightarrow \mu/2$ (for the second term on the r-h-s of Eq. (7)). But based on our previous analysis, this simultaneous condition is very unlikely to happen for an arbitrary function $D(x)$. Furthermore, for some very specific possible values of $L(t)$, instantly the sum of the two terms on the r-h-s of Eq. (7) could become zero. However, this exact cancelation would cease at subsequent times as $L(t)$ varies.

The corresponding Fokker-Planck equation for the Langevin equation (7) in the Stratonovich approach is given by [47]

$$\begin{aligned} \frac{\partial \rho(x, t)}{\partial t} = & -\frac{\partial}{\partial x} \left[\left(a |G(x)|^{\mu-1} + b |G(x)|^{\mu} \frac{dD(x)}{dx} \right) D(x) \rho(x, t) \right] + \\ & b \frac{\partial^2}{\partial x^2} [|G(x)|^{\mu} D^2(x) \rho(x, t)], \end{aligned} \quad (9)$$

where $\rho(x, t)$ is the probability density function (PDF).

III. EXACT SOLUTIONS AND ANALYSES OF EQ. (9)

In this section we shall address the models described by Eq. (9). In doing so, we need to consider two distinct situations, $\mu \neq 2$ and $\mu = 2$. Exact solutions are then derived by means of variable transformations and by using, respectively, the similarity method for the former and the Fourier transform method for the latter. More concrete and detailed examples are discussed in Sec. IV. Next, we will assume $G(\pm\infty) \rightarrow \pm\infty$.

A. The case $\mu \neq 2$: Solutions from the similarity method

Equation (9) can be written as follows:

$$\frac{\partial \rho(x, t)}{\partial t} = -a \frac{\partial}{\partial x} \left[|G(x)|^{\mu-1} D(x) \rho(x, t) \right] + b \frac{\partial}{\partial x} \left[D(x) \frac{\partial}{\partial x} (|G(x)|^\mu D(x) \rho(x, t)) \right]. \quad (10)$$

Thus, from the transformations

$$\bar{x} = G(x), \quad \bar{\rho}(\bar{x}, t) = D(x) \rho(x, t), \quad (11)$$

Eq. (10) reduces to

$$\frac{\partial \bar{\rho}(\bar{x}, t)}{\partial t} = -a \frac{\partial}{\partial \bar{x}} \left[|\bar{x}|^{\mu-1} \bar{\rho}(\bar{x}, t) \right] + b \frac{\partial^2}{\partial \bar{x}^2} \left[|\bar{x}|^\mu \bar{\rho}(\bar{x}, t) \right]. \quad (12)$$

The above equation is invariant under the rescaling (with γ arbitrary)

$$\bar{x} \rightarrow \epsilon \bar{x}, \quad t \rightarrow \epsilon^{2-\mu} t, \quad \bar{\rho} \rightarrow \epsilon^\gamma \bar{\rho}. \quad (13)$$

Thus, we can employ the similarity solution method [52, 87, 88] to address Eq. (12).

For $\bar{\rho}(\bar{x}, t) = t^{-\alpha} \Phi(z)$ and $z = \bar{x}/t^\alpha$, with the scaling exponent $\alpha = 1/(2 - \mu)$, Eq. (12) reduces to the ordinary differential equation (for \mathcal{A} a constant)

$$b \frac{d}{dz} \left(|z|^\mu \Phi \right) + \left(\alpha z - a |z|^{\mu-1} \right) \Phi = \mathcal{A}. \quad (14)$$

By setting $\mathcal{A} = 0$ in Eq. (14) (for our purposes here we do not need to address the $\mathcal{A} \neq 0$ case), it readily follows that

$$\Phi(z) = C \frac{|z|^{\frac{a}{b} \text{sign}(z) - \mu}}{b} \exp \left[-\frac{|z|^{2-\mu}}{b(2-\mu)^2} \right], \quad (15)$$

where C represents the normalization constant. Therefore, a solution for Eq. (9) in the case of $\mu \neq 2$ reads

$$\rho(x, t) = C \frac{|G(x)|^{\frac{a}{b} \text{sign}(G(x)) - \mu}}{b D(x) t^{\frac{1-\mu + \frac{a}{b} \text{sign}(G(x))}{2-\mu}}} \exp \left[-\frac{|G(x)|^{2-\mu}}{b(2-\mu)^2 t} \right]. \quad (16)$$

Note that the spatial asymmetry is manifested in Eq. (16) through the term $\text{sign}[G(x)]$. For a vanishing a , such asymmetry disappears. We highlight that the PDF in Eq. (16) can display a broad range of behaviors depending on $D(x)$ and the corresponding $G(x)$.

The normalization condition for $\rho(x, t)$ is the same as that for $\Phi(z)$, so that we should have

$$\int_{-\infty}^{\infty} \rho(x, t) dx = \int_{-\infty}^{\infty} \Phi(z) dz = 1, \quad (17)$$

since $G(\pm\infty) \rightarrow \pm\infty$. From Eq. (17) we obtain the following normalization constant by formal integration

$$C = \frac{(b(2-\mu)^2)^{\frac{1}{2-\mu}}}{|2-\mu| \left((b(2-\mu)^2)^{-\frac{a}{b(2-\mu)}} \Gamma \left[\frac{1-\mu-\frac{a}{b}}{2-\mu} \right] + (b(2-\mu)^2)^{\frac{a}{b(2-\mu)}} \Gamma \left[\frac{1-\mu+\frac{a}{b}}{2-\mu} \right] \right)}, \quad (18)$$

where $\Gamma[\cdot]$ denotes the Gamma function. We find that the PDF (16) is not normalizable for $1 \leq \mu < 2$ (actually, the similarity method is not the most appropriate method to treat the $\mu = 2$ case, see next section). Similarly, one of the following two restrictions must also be verified for a proper C :

- If $\mu < 1$, then for a finite C we further must have $\mu < 1 - |a|/b$,
- If $\mu > 2$, then for a finite C we further must have $\mu > 1 + |a|/b$.

Usually, for an arbitrary $D(x)$ the computation of the n -moment, given by $\langle x^n(t) \rangle$, is not an easy task. On the other hand, the generalized n -moment $\langle G^n(x) \rangle$ is far more amenable to calculations. In order to obtain the generalized n -moment we take the whole space $(-\infty, \infty)$ for x , supposing a generic $D(x) \geq 0$ (but we must notice that special cases might be simpler to handle, for instance, $G(x) = x$ if $D(x) = 1$ then we recover the ordinary n -moment $\langle x^n(t) \rangle = \langle G^n(x(t)) \rangle$). Recall the extra condition, $G(\pm\infty) \rightarrow \pm\infty$. In this way, from $\int_{-\infty}^{\infty} G^n(x) \rho(x, t) dx$ we have

$$\langle G^n(x) \rangle = C |2-\mu| (b(2-\mu)^2)^{\frac{n-1-\frac{a}{b}}{2-\mu}} t^{\frac{n}{2-\mu}} \times \left((-1)^n \Gamma \left[\frac{n+1-\mu-\frac{a}{b}}{2-\mu} \right] + (b(2-\mu)^2)^{\frac{2\frac{a}{b}}{2-\mu}} \Gamma \left[\frac{n+1-\mu+\frac{a}{b}}{2-\mu} \right] \right). \quad (19)$$

Repeating the same type of analysis for Eq. (19) as previously, we find that the generalized n -moment is finite only if

- $\mu < 2$: $n+1 > \mu + |a|/b$,
- $\mu > 2$: $n+1 < \mu - |a|/b$.

B. The case $\mu = 2$

For the particular case of $\mu = 2$ we employ variable transformations and Fourier transform method. Now we rewrite Eq. (9) as follows.

$$\frac{\partial \rho(x, t)}{\partial t} = -\frac{\partial}{\partial x} \left[(a - b \operatorname{sign}(G(x))) H(x) \rho(x, t) \right] + b \frac{\partial}{\partial x} \left[H(x) \frac{\partial}{\partial x} (H(x) \rho(x, t)) \right], \quad (20)$$

where $H(x) = |G(x)| D(x)$. For simplicity, we restrict ourselves to the case where $\text{sign}(G(x))$ assumes a unique value. Considering

$$\frac{dx^*}{dx} = \frac{1}{H(x)} \quad \text{and} \quad \rho^*(x, t) = H(x) \rho(x, t), \quad (21)$$

we obtain the following Fokker-Planck equation:

$$\frac{\partial \rho^*(x^*, t)}{\partial t} = -\frac{\partial}{\partial x^*} [(a - b \text{sign}(G(x))) \rho^*(x^*, t)] + b \frac{\partial^2}{\partial x^{*2}} \rho^*(x^*, t); \quad (22)$$

its solution is obtained from the Fourier transform method supposing the initial condition $\rho^*(x^*, 0) = \delta(x^* - x_0^*)$. The final result is then [85]

$$\rho(x, t) = \frac{C}{\sqrt{4\pi b t} H(x)} \exp \left[-\frac{(x^*(x) - x_0^* - (a - b \text{sign}(G(x))) t)^2}{4 b t} \right], \quad (23)$$

where C is the normalization constant.

We should remark that the PDF in Eq. (23) is also the solution for the case of zero drift, but for the position coordinate x^* translated by

$$x^*(x) \rightarrow x^*(x) - (a - b \text{sign}(G(x))) t. \quad (24)$$

C. The qualitative dynamical evolution of the deterministic and stochastic models in the parameters space

In the previous sections we have analyzed the features of the deterministic and stochastic models in terms of ranges of values for the parameters. In particular, we have unveiled that in most instances, the non-linear deterministic models of Eq. (1) display rather straightforward (monotonous) trends. In fact, they would require specific conditions — both for the set $\Lambda = \{a, b, \mu\}$ as well for the properties of $D(x)$ and $G(x)$ — so to yield a more diverse dynamics for $x(t)$, say oscillating between two extrema, x_{min} and x_{man} , instead of approaching a fixed point \bar{x} in finite time or asymptotically evolving towards $\pm\infty$.

Conversely, by adding white noise to our original problem, we have obtained a non-linear Langevin equation, given by Eq. (7). In this case dynamical traps are far more rare and the evolution of the now stochastic $x(t)$ is not affected by most of the restrictions discussed for the deterministic case in Sec. II A. However, rather than addressing in detail such stochastic microscopic variable, we have followed the standard procedure of considering

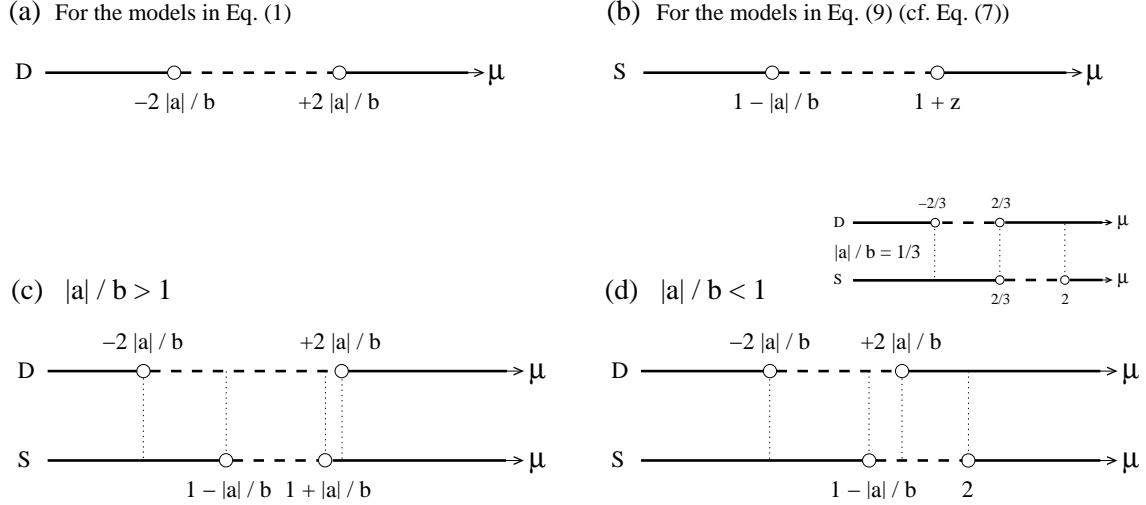


FIG. 3: (a) In the absence of dynamical traps (see Sec. II A), for the deterministic models D the μ parameter intervals for which the trajectories either steadily tend to infinity (dashed segment, of length $\Delta\mu_D = 4|a|/b$) or have a richer oscillating behavior, confined to a certain x spatial region (continuous semi-lines). (b) For the stochastic models S, the continuous semi-lines (dashed segment, of length $\Delta\mu_S = z + |a|/b$) indicate the μ parameter values for which $\rho(x, t)$ has (has not) well-behaved analytic expressions. Here $z = \max(1, |a|/b)$. Defining $r = \Delta\mu_D/\Delta\mu_S$, the μ interval for D leading to diverging trajectories is always longer than those for S presenting no proper $\rho(x, t)$ solutions provided $|a|/b > 1/3$. Indeed, (c) $r = 2$ for $|a|/b > 1$ and (d) $r = 4(|a|/b)/(1 + |a|/b) > 1$ if $1 > |a|/b > 1/3$ (the inset depicts the $|a|/b = 1/3$ case).

the associated probability density function $\rho(x, t)$, seeking for general non-trivial solutions displaying spatial asymmetry. For instance, notice that relevant changes of behavior for ρ arise depending on the term $\text{sign}(G(x))$ appearing in Eq. (16) (explicit examples in the next section).

Thus, keeping in mind the obvious conceptual differences between the physical meaning of $x(t)$ governed by Eq. (1) and $\rho(x, t)$ by Eq. (10), one can qualitatively contrast their dynamics considering the ranges of $\Lambda = \{a, b, \mu\}$ (see Fig. 3 (a) and (b)), which in one hand may result in simple monotonic evolution for the deterministic systems, but on the other hand might allow phenomenologically much more diverse behavior for the stochastic models (cf., Eq. (16)). This kind of comparison can be viewed as a heuristic (but not sensibly departing from more rigorous approaches in the literature, e.g., as those in [92, 93]) or even an operational way of inferring how stochasticity can lead to the emergence of complexity

[94] in certain classes of processes such as [95, 96]: dynamics in networks, lasing in noisy media, pattern-formation, granular matter nucleation and ecological interactions, to cite a few examples.

So we need to address only the instances where $x(t)$ in Eq. (1) can asymptotically diverge since the scarcity of dynamical traps for Eq. (7) has already been discussed (see the paragraph following Eq. (8) in Sec. II B). We restrict the analysis to $\mu \neq 2$. For our purposes we rewrite Eq. (7) as

$$\frac{dx(t)}{dt} = \mathcal{F}(x) \left(\mathcal{G}(x) + L(t)/\sqrt{b} \right), \quad (25)$$

where $\mathcal{F}(x) = b|G(x)|^{\mu/2} D(x) \geq 0$ and $\mathcal{G}(x) = (a/b - (\mu/2) \text{sign}(G(x))) |G(x)|^{\mu/2-1}$. We also recall the condition (i) in Sec. II A, namely,

$$|a|/b > |\mu|/2. \quad (26)$$

For it (cf. Fig. 3 (a)), regardless of $G(x)$ the dynamical evolution of the deterministic models in the absence of traps are monotonic, i.e., $x(t)$ invariably just increases or just decreases with t . Moreover, by inspecting $\mathcal{G}(x)$ in Eq. (25) and considering the relation in Eq. (26) it follows that $\mathcal{G}(x)$ is either always positive (+) or always negative (-). So, in the long run $x(t)$ should not diverge (i.e., in average not evolving towards $\pm\infty$) only if the fluctuations from $L(t)/\sqrt{b}$ could refrain this biased evolution of $x(t)$ driven by $\mathcal{G}(x)$. Observe that in such a context, $x(t)$ does resemble a random walk, but with a spatial bias in a given direction. In other words, in this situation — which we call the non-stabilization condition — the added noise cannot confine the systems. We shall emphasize the known fact [97] that for a non-linear Langevin equation, certain characteristics of the resulting non-linear trajectories, noticeably divergence [98, 99], may hinder a proper PDF description via a linear Fokker-Planck equation (for a comprehensive discussion see, e.g., [100]). Particularly, it poses important issues related to stability and solvability of the latter [99, 101].

Then, first consider $|a|/b > 1$. When $\mu > 2$ ($\mu < 1$), from Eq. (26) the deterministic models are monotonic for $2 < \mu < 2|a|/b$ ($-2|a|/b < \mu < 1$), tending to $\pm\infty$ if there are no dynamical traps along the way. But when $\mu > 2$ ($\mu < 1$), the stochastic models are well-behaved for $\mu > 1 + |a|/b$ ($\mu < 1 - |a|/b$), Sec. III A. Hence, stabilization through the addition of white noise is attained in the “extra” intervals $1 + |a|/b < \mu \leq 2|a|/b$ and $-2|a|/b \leq \mu < 1 - |a|/b$, Fig. 3 (c), representing a considerable range increasing along μ of

$\Delta\mu = 2|a|/b$. In the remaining interval $1 - |a|/b < \mu < 1 + |a|/b$ for the stochastic models — in which Eq. (1) also leads to diverging trajectories — the function $\mathcal{G}(x)$ in Eq. (25) has always the same sign and the noise is not enough to avoid the asymptotic natural leaning. Consequently, for $1 - |a|/b < \mu < 1 + |a|/b$ the mentioned non-stabilization condition applies.

Second, assume $|a|/b < 1$. The distinction is that now the stochastic models have no solutions for $1 - |a|/b < \mu < 2$ (instead of $1 - |a|/b < \mu < 1 + |a|/b$). In this way, the analysis for the left limits are akin to $\mu < 1$ above, compare Fig. 3 (c) and (d). Thus, we can focus only on the right limits. Observe that in the range $1 - |a|/b < \mu < 2|a|/b$, Fig. 3 (d), the previous non-stabilization condition takes place. On the contrary, although the deterministic systems are not diverging in the interval $2|a|/b < \mu < 2$, the stochastic ones have no solutions. For the time being we have not found a more conceptual explanation — mathematically, they are those in Sec. III A — for such result (hopefully, it will be elucidated in a forthcoming contribution). But the point is that by the inclusion of noise, the interval of diverging trajectories for the deterministic models, $4|a|/b$, is larger than the interval of non-normalizable solutions for the stochastic models, $1 + |a|/b$, whenever $|a|/b > 1/3$. We remark that $|a|/b = 1/3$ is the threshold to exist an overlap between the intervals $(-2|a|/b, +2|a|/b)$ and $(1 - |a|/b, 2)$, respectively, for the deterministic and stochastic models, see the inset of Fig. 3 (d). The qualitative reason for this borderline $|a|/b = 1/3$ value also requires future investigations.

IV. SOME SPECIFIC EXAMPLES FOR THE STOCHASTIC MODEL

Next we illustrate by means of simple, but representative, examples some trends of the PDF ρ 's presented in Sec. III. In Sec. IV A we consider $\mu \neq 2$ and $D(x) = 1$. This is an interesting choice because in this case the generalized n -moment reduces to the standard one ($\langle x^n \rangle$). In Sec. IV B we address $\mu = 2$. In particular, for a specific $D(x)$ we show that our system relates to important population growth models in the literature.

A. The case of $\mu \neq 2$ and $D(x) = 1$

For $D(x) = 1$ we have $G(x) = x + \text{constant}$. For simplicity we set such constant to zero. We just comment that depending on a , b and μ (and the initial condition x_0), the dynamical

system can either become stationary or diverging.

In Eq. (7), $|G(x)|^{\mu-1} = |x|^{\mu-1}$ and $|G(x)|^{\mu/2} = |x|^{\mu/2}$ give rise to distinct power-law functions. The normalized PDF reads (for C in Eq. (18))

$$\rho(x, t) = C \frac{|x|^{\frac{a}{b}\text{sign}(x)-\mu}}{b t^{\frac{1-\mu+\frac{a}{b}\text{sign}(x)}{2-\mu}}} \exp\left[-\frac{|x|^{2-\mu}}{b(2-\mu)^2 t}\right]. \quad (27)$$

It is interesting to note that the PDF given by Eq. (27), for $\mu = a/b$ and $\mu < 1$, is composed of a stretched or compressed Gaussian distribution and a generalized Weibull distribution. This dual functional form suggests that the system described by Eq. (7) may be used to model processes resulting from different dynamical drives.

The n -moment can be obtained from Eq. (19), yielding

$$\begin{aligned} \langle x^n \rangle = & C |2-\mu| (b(2-\mu)^2)^{\frac{n-1-\frac{a}{b}}{2-\mu}} \left((-1)^n \Gamma\left[\frac{n+1-\mu-\frac{a}{b}}{2-\mu}\right] \right. \\ & \left. + (b(2-\mu)^2)^{\frac{\frac{2a}{b}}{2-\mu}} \Gamma\left[\frac{n+1-\mu+\frac{a}{b}}{2-\mu}\right] \right) t^{\frac{n}{2-\mu}} \end{aligned} \quad (28)$$

In the particular case of $a = 0$, the PDF in Eq. (27) reduces to

$$\rho(x, t) = \frac{(b(2-\mu)^2)^{\frac{1}{2-\mu}} |x|^{-\mu}}{2b|2-\mu| \Gamma\left[\frac{1-\mu}{2-\mu}\right] t^{\frac{1-\mu}{2-\mu}}} \exp\left[-\frac{|x|^{2-\mu}}{b(2-\mu)^2 t}\right], \quad (29)$$

and Eq. (28) results in (with $C_0 = C|_{a=0}$)

$$\langle x^n \rangle = C_0 |2-\mu| (b(2-\mu)^2)^{\frac{n-1}{2-\mu}} \Gamma\left[\frac{n+1-\mu}{2-\mu}\right] ((-1)^n + 1) t^{\frac{n}{2-\mu}}. \quad (30)$$

One can see that $\langle x^n \rangle$ in Eq. (30) is zero for n an odd number, in accordance with the symmetric PDF in Eq. (29). In particular, its second moment goes with $t^{2/(2-\mu)}$, hence it can describe superdiffusive, normal and subdiffusive, processes respectively for, $0 < \mu < 1$, $\mu = 0$ and $\mu < 0$. Further, for $\mu > 2$ the system describes localized processes.

Generally, the PDF in Eq. (27) represents a system with a power-law potential of order higher than 2 when $\mu > 2$ and with a spatial asymmetry associated with the term $a \text{sign}(x)$, or (with $a \neq 0$ and $b\mu/2 - a \text{sign}(x) > 0$)

$$V(x) \sim \frac{(b\mu/2 - a \text{sign}(x))}{\mu} |x|^\mu. \quad (31)$$

Thus, the parameter $|a|$ determines the degree of asymmetry, with $a = 0$ leading to a totally symmetric PDF, Eq. (29).

The solution given by Eq. (27) is not valid for $\mu = 2$. Nonetheless, we can take $\mu \sim 2$, so that $|G(x)|^{\mu-1}$ (related to the non-linear drift and with the asymmetry term $\text{sign}(G(x))$) and $|G(x)|^{\mu/2}$ (related to the white noise coefficient) in Eq. (7) are both approximately linear in $|G(x)|$. In this case the $V(x)$ in Eq. (31) with $\mu \sim 2$ fairly represents the usual symmetric (asymmetric) harmonic potential for $a = 0$ ($a \neq 0$ and $b/2 > |a|$).

We can also compare the PDF in Eq. (29) with that one obtained from Eq. (7), but without drift and derived from different prescriptions, or (see the ref. [52])

$$\rho(x, t) = \frac{|x|^{-(1-\lambda)\mu}}{2|2-\mu|^{\frac{-(1-2\lambda)\mu}{2-\mu}} \Gamma\left[\frac{1-(1-\lambda)\mu}{2-\mu}\right] (bt)^{\frac{1-(1-\lambda)\mu}{2-\mu}}} \exp\left[-\frac{|x|^{2-\mu}}{b(2-\mu)^2 t}\right]. \quad (32)$$

Here $0 \leq \lambda \leq 1$ is the prescription parameter, for $\lambda = 1/2$ yielding the Stratonovich's and $\lambda = 0$ the Ito's. The n -moment related to the PDF (32) is given by

$$\langle x^n(x) \rangle = \frac{(b(2-\mu)^2)^{\frac{n}{2-\mu}} \Gamma\left[\frac{n+1-(1-\lambda)\mu}{2-\mu}\right] t^{\frac{n}{2-\mu}}}{\Gamma\left[\frac{1-(1-\lambda)\mu}{2-\mu}\right]}, \quad (33)$$

where n is an even number. Observe that Eq. (32) coincides with Eq. (29) for $\lambda = 0$ (the Ito prescription). This follows directly from the fact that for the Fokker-Planck equation in Eq. (9), the drift term vanishes since for $D(x) = 1$ we have $dD(x)/dx = 0$. Moreover, the n -moment in Eq. (33) has similar behavior to that one given by Eq. (30) for even numbers.

All these findings show that there are a large class of systems displaying the same n -moment trends.

Finally, graphs of Eq. (27) for distinct parameter values (all with $a > 0$) and at different time instants t are depicted in Figs. 4–7. For $a \rightarrow -a$ we get a specular image, about $x = 0$, of the observed profiles. Since $G(x) = x$, which is anti-symmetric in x , all the plots display an imbalance regarding positive and negative x 's, hence overall with $\rho(x < 0)$ much greater than $\rho(x > 0)$. Also, the imbalance tends to be stronger for greater $|a|$'s. For Figs. 4–6 (7 (a) and 7 (b)) we have $\xi = \mu - 1 > 0$ ($\xi = 1 - \mu > 0$), so that $|G(x)|^{\mu-1} D(x) = |x|^\xi$ ($|G(x)|^{\mu-1} D(x) = 1/|x|^\xi$). This explains why the corresponding PDFs are very small (very large) for x approaching zero. From the plots for $\mu > 2$ we see that as t increases, the distributions tend to concentrate around the origin. We have checked this is likewise the case for the examples with $\mu < 1$ (not shown), but then with such concentration taking place slower in time. As a last remark, provided a and b are the same and the values of the associated μ 's do not differ much, we have not detected relevant qualitatively differences

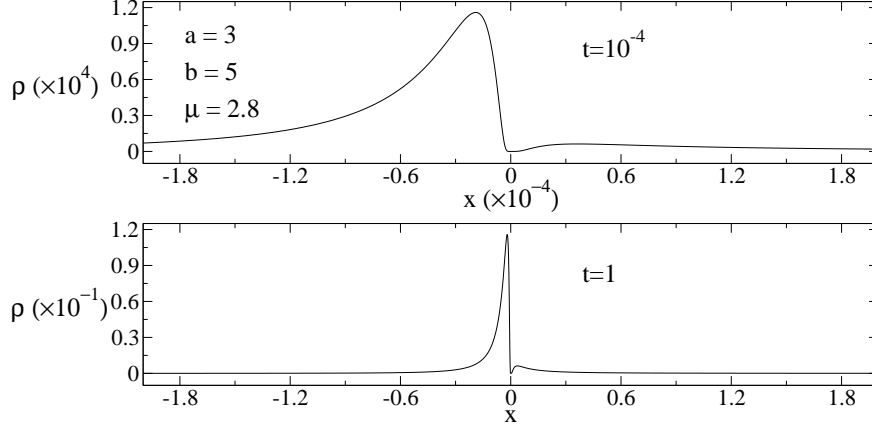


FIG. 4: For the case of $D(x) = 1$, the resulting PDF, Eq. (27), at two time instants, $t = 1$ and the very short $t = 10^{-4}$ (on purpose, to illustrate the shape of the initial PDF). For the parameters a , b and μ considered, $\mu > 2 > 1 + a/b > 2a/b$, thus not belonging to the monotonic behavior (i) for the dynamical system. Although the distribution is considerably higher for $x < 0$, it is still noticeable for x positive, but only in the origin vicinity. In the plots, both ρ and x have been rescaled so to facilitate a direct comparison between the curves shapes. Notice that ρ is spatially much more concentrated at $t = 1$ than at $t = 10^{-4}$.

among the ρ 's either when $2a/b < \mu < 1 - a/b$ or when $\mu < 2a/b < 1 - a/b$ if $\mu < 1$ and when $\mu > 1 + a/b > 2a/b$ or when $2a/b > \mu > 1 + a/b$ if $\mu > 2$.

B. Some examples for $\mu = 2$

We finally consider the solution in Eq. (23). For $H(x) = \sqrt{h}$, with h a positive constant, we have $x^*(x) = x/\sqrt{h}$, $|G(x)| = \exp[\pm x/\sqrt{h}]$ and $D(x) = \sqrt{h} \exp[\mp x/\sqrt{h}]$. In this case, the PDF in Eq. (23) recovers the well-known ρ for a Brownian motion with a load force, whose expression is [79]

$$\rho(x, t) = \frac{1}{\sqrt{4\pi b h t}} \exp \left[-\frac{(x - x_0 - \sqrt{h}(a - b)t)^2}{4 b h t} \right]. \quad (34)$$

A particularly interesting situation, relating to other models in the literature, results from $H(x)$ given by

$$H(x) = \frac{(K^\alpha - x^\alpha) x}{\beta K^\alpha - (\beta - \alpha) x^\alpha}, \quad (35)$$

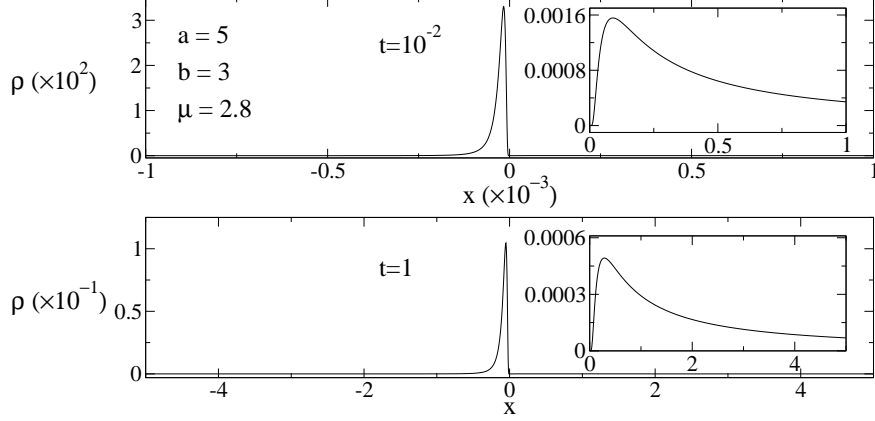


FIG. 5: Similar plots as in Fig. 4, but for the parameters values such that $2a/b > \mu > 1 + a/b > 2$. Hence, the corresponding dynamical system does belong to the monotonic behavior class (i). Since now the PDFs are very small for x positive, the insets show proper blow ups for $x > 0$. Again, ρ is spatially much more concentrated at $t = 1$ than at $t = 10^{-2}$.

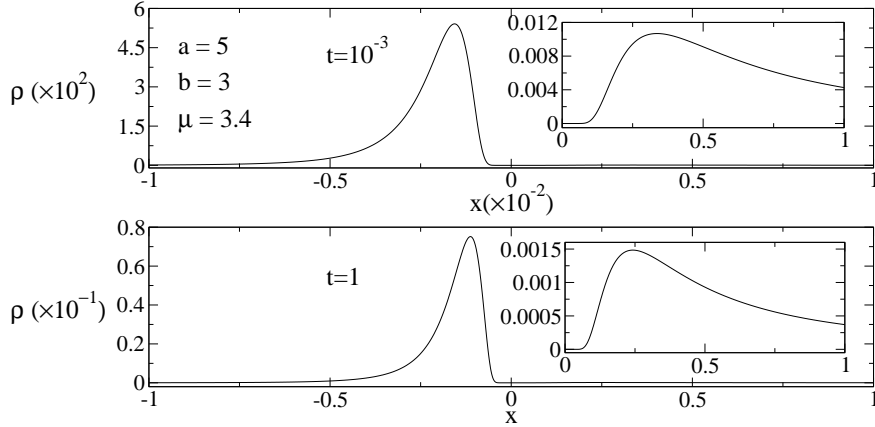


FIG. 6: Similar plots as in Fig. 5, but for the parameters satisfying $\mu > 2a/b > 1 + a/b > 2$. Thus, as in Fig. 4, not belonging to the monotonic behavior (i) for the dynamical system. The PDF is spatially much more concentrated at $t = 1$ than at $t = 10^{-3}$.

such that

$$D(x) = \frac{K^\beta}{K^\alpha} \frac{(K^\alpha - x^\alpha)^2 x^{1-\beta}}{(\beta K^\alpha - (\beta - \alpha) x^\alpha)}, \quad G(x) = \frac{(x/K)^\beta}{1 - (x/K)^\alpha}. \quad (36)$$

In this case, the PDF in Eq. (23) is related to the population growth model proposed in [22] (see also [20]). More specifically, $0 \leq x(t) \leq K$ is the number of alive individuals in a population at time t , $r = a - b \text{sign}(G(x)) = a - b$ is the intrinsic growth rate with $a > b$, and K is the carrying capacity. For simplicity, the parameters β and α are restricted to

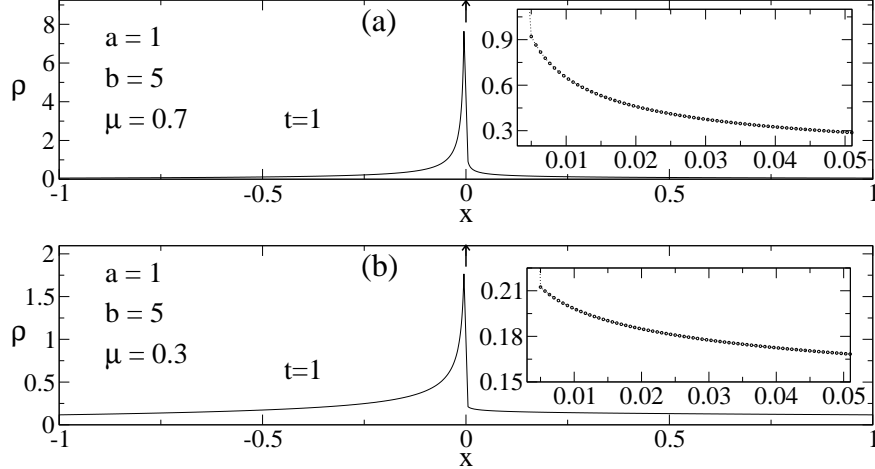


FIG. 7: For $D(x) = 1$, the PDF in Eq. (27) at $t = 1$ with $a = 1$, $b = 5$ and two values of $\mu < 1$. (a) $\mu = 0.7$, thus $2a/b < \mu < 1 - a/b < 1$. (b) $\mu = 0.3$, thus $\mu < 2a/b < 1 - a/b < 1$. The arrows indicate that although integrable, these ρ 's tend to $+\infty$ at the origin. The insets give details of the distributions for $x > 0$ very close to the origin. These PDF's tend to be more concentrate as t increases, plots not shown.

real non-negative values. In fact, the system described by Eqs. (7) and (35) encompasses classical growth models such as the Verhulst logistic ($\beta = 1$ and $\alpha = 1$), Gompertz ($\beta = 0$ and $\alpha \rightarrow 0$), Shoener ($\beta = 0$ and $\alpha = 1$), Richards ($\beta = 0$ and $0 < \alpha < \infty$) and Smith ($0 \leq \beta < \infty$ and $\alpha = 1$) [18–25]. Also, for $\beta = \alpha = 1$ the present framework has been employed in the study of population genetics [15].

In formulating the above mentioned models through the present approach, some care is necessary concerning the normalization constant. For instance, to avoid a time dependent C (implying in a non-conservation of probability along t), the limits of integration for ρ , $x_i^*(x = 0)$ and $x_f^*(x = K)$, should not be finite. This is determined from (recall that $dx^*/dx = 1/H(x)$)

$$x^* = \ln \left[\frac{(x/K)^\beta}{1 - (x/K)^\alpha} \right]. \quad (37)$$

As an example we consider the Shoener and Richards models (both with $\beta = 0$). They cannot be constructed under the present procedure once the lower limits have finite values. Indeed, for $\beta = 0$ and $\alpha > 0$ we get $x^* = -\ln[1 - (x/K)^\alpha]$, so that x_i^* is zero for $x = 0$.

For $\beta, \alpha \neq 0$ we have $x^*(x \rightarrow 0) \rightarrow -\infty$ and $x^*(x \rightarrow K) \rightarrow \infty$. Thus, from Eq. (23) we

find $C = 1$ and the PDF yields (with $t_0 = 0$)

$$\rho(x, t) = \frac{1}{\sqrt{4\pi b t} H(x)} \exp \left[-\frac{(x^*(x) - x_0^* - (a - b)t)^2}{4 b t} \right]. \quad (38)$$

In general x_0^* is considered finite (except for $\alpha \rightarrow 0$). Thus, one should exclude a population that is initially null ($x_0 \rightarrow 0$) or that is already at its maximum possible value established by K ($x_0 \rightarrow K$)

V. CONCLUSION

In this contribution we have considered a set of models with asymmetric space-dependent drifts. For the deterministic case, we have identified their temporal evolution features in the parameters space $\Lambda = \{a, b, \mu\}$ and also in terms of certain general properties of the driven function $D(x)$ (and of its primitive integral $G(x)$). We have shown the deterministic models display rather simple behavior in a large region of Λ .

Then, by adding the Gaussian white noise to such class of problems we have obtained nonlinear Langevin equations, whose associated Fokker-Planck equations have been solved through the similarity method or Fourier transform method. In the subset of Λ where the obtained ρ 's are well behaved, we have discussed the dynamical richness emerging from these PDFs. For instance, conceivably they could be used to study anomalous diffusion, with applications in different processes as population growth models.

By comparing the two families of models in Λ , we have unveiled the effects of introducing stochasticity and the mechanisms allowing the qualitative changes observed in the systems dynamics. Concretely, we have found that for some regions of Λ , although the trajectories of the deterministic models are trivial, i.e., either fall into fixed points or evolve to $\pm\infty$, in the stochastic case they become stable. By stable we mean the orbits no longer diverge or go into sinks, instead the velocity function $dx(t)/dt$ may have a complex behavior, but in such a way to assure that the particle is confined to a certain limited region of space and do not stop moving.

In conclusion, to understand how the natural laws, so economical in number and so simple in structure, determine the huge behavioral richness perceived in the physical world is one of the great challenges in science [1–4, 7]. It has been long known that random inputs [44, 45], in otherwise deterministic systems, can account for part of such multiplicity [28–32].

Although much progress has been achieved, the effects promoting diversity in noise-assisted dynamical evolution are very far from a complete description (see, for instance, [40–43]). We hope that at least for some interesting cases, the present theoretical results can help to shed some light into this crucial query.

Acknowledgments

We would like to thank G. V. Viswanathan for a critical reading of earlier versions of the present manuscript and M. W. Beims for helpful discussions about stabilization processes in dynamical systems. MGEL acknowledges financial support from CAPES (via the CAPES PRINT-UFPR program “Efficiency in uptake, production and distribution of photovoltaic energy distribution as well as other renewable sources of renewable energy sources”) Grant No. 88881.311780/2018-00 and CNPq for the research Grant No. 304532/2019-3. YBM acknowledges CAPES for a PhD scholarship. CLH is supported in part by the National Science and Technology Council (NSTC) of the Republic of China under Grant No. NSTC 112-2112-M-032-007.

Appendix A: The implicit analytic solution for the dynamical system represented by Eqs. (1) and (2)

Our dynamical system can be solved analytically by considering the successive spatial intervals $I_n^{(\pm)} = (c_n^{(\pm)}, d_n^{(\pm)})$ — with $\text{sign}[G(x \in I_n^{(\pm)})] = \pm 1$ — to which $x_n(t)$ belongs to at the corresponding time intervals \mathcal{I}_n . The full trajectory $x(t)$ is then given by the proper concatenation of these piecewise $x_n(t)$ for $t \in \mathcal{I}_n$.

So, here we discuss only the functional form of $x(t)$ in an arbitrary $I^{(+)}$ or $I^{(-)}$ with $t \in \mathcal{I} = (t_0, T)$ and for simplicity assuming the starting point $x_0 = x(t_0)$ in the interior of $I^{(\pm)}$. We observe that in concrete instances, one also should correctly deal with the behavior of $x(t)$ in crossing from a spatial interval $I^{(\pm)}$ to $I^{(\mp)}$. But as seen in Sec. II A, this demands to know the exact form of $D(x)$.

For the following let us set $G_0 = G(x_0)$ and denote by \tilde{G} the formal inverse function of G . Hence, for all x it holds that $\tilde{G}(G(x)) = x$.

1. $x(t) \in I^{(+)}$ for the time interval $t \in (t_0, T)$

In this case $G(x) \geq 0$ (with the equality only at the borders of $I^{(+)}$) and

$$\frac{dx(t)}{dt} = cG(x)^{\mu-1} D(x), \quad (\text{A1})$$

with $c = a - b\mu/2 \neq 0$ (of course, $c = 0$ leads to a trivial solution). Note that $G_0 > 0$.

Then, by the direct integration of Eq. (A1) taking into account Eq. (2), we find that ($t \in (t_0, T)$)

$$\begin{aligned} x(t) &= \tilde{G}([c(2-\mu)(t-t_0) + G_0^{2-\mu}]^{1/(2-\mu)}), & \text{for } \mu \neq 2, \\ x(t) &= \tilde{G}(G_0 \exp[c(t-t_0)]), & \text{for } \mu = 2. \end{aligned} \quad (\text{A2})$$

2. $x(t) \in I^{(-)}$ for the time interval $t \in (t_0, T)$

Now $G(x) \leq 0$ (with the equality only at the borders of $I^{(-)}$) and

$$\frac{dx(t)}{dt} = d[-G(x)]^{\mu-1} D(x), \quad (\text{A3})$$

with $d = a + b\mu/2 \neq 0$ (again, the $d = 0$ case is trivial). Observe that $G_0 < 0$.

Finally, by integrating Eq. (A3) using Eq. (2) we get ($t \in (t_0, T)$)

$$\begin{aligned} x(t) &= \tilde{G}(-[d(\mu-2)(t-t_0) + (-G_0)^{2-\mu}]^{1/(2-\mu)}), & \text{for } \mu \neq 2, \\ x(t) &= \tilde{G}(G_0 \exp[-d(t-t_0)]), & \text{for } \mu = 2. \end{aligned} \quad (\text{A4})$$

-
- [1] Nakamura E R, Kudo K, Yamakawa O and Tamagawa Y (Eds.) 1997 *Complexity and Diversity* (Tokyo: Springer-Verlag)
- [2] Page S E 2011 *Diversity and Complexity* (Princeton: Princeton University Press)
- [3] Rand D A 1994 *Philos. Trans. Royal Soc. A.* **348** 497-514
- [4] Rand D A and Wilson H B 1995 *Proc. R. Soc. Lond. B* **259** 111-117.
- [5] Cugliandolo L F 2015 *C. R. Phys.* **16** 257-266
- [6] Mayer P, Bissig H, Berthier L, Cipelletti L, Garrahan J P, Sollich P and Trappe V 2004 *Phys. Rev. Lett.* **93** 115701
- [7] Stankovski T, Pereira T, McClintock P V E and Stefanovska A 2017 *Rev. Mod. Phys.* **89** 045001
- [8] Agafonov S A 2005 *J. Math. Sci.* **125** 556
- [9] Cumming G S 2011 *Spatial Resilience in Social-Ecological Systems* (Dordrecht: Springer)
- [10] Lowery N V and Ursell T 2019 *Proc. Nat. Acad. Sci.*, **116** 379-388
- [11] Edri Y, Meron E and Yochelis A 2020 *Chaos* **30** 023120
- [12] Krause A L, Klika V, Woolley T E and Gaffney E A 2018 *Phys. Rev. E* **97** 052206
- [13] Edri Y, Meron E and Yochelis A 2020 *Physica D* **410** 132501
- [14] Sun J W 2021 *Nonlinearity* **34** 5434
- [15] Kimura M 1964 *J. Appl. Probability* **1** 177-232
- [16] Liang Y J, Allen Q Y, Chen W, Gatto R G, Colon-Perez L, Mareci T H and Magin R L 2016 *Commun. Nonlinear Sci. Numer. Simul.* **39** 529-537
- [17] Fa K S 2017 *J. Stat. Mech.* **2017** 033207
- [18] Aquino G, Bologna M and Calisto H 2010 *Eurphys. Lett.* **89** 50012
- [19] Jackson P J, Lambert C J, Mannella R, Martano P, McClintock P V E and Stocks N G 1989 *Phys. Rev. A* **40** 2875
- [20] Fa K S 2012 *Ann. Phys.* **327** 1989-1997
- [21] Richards F J 1959 *J. Exp. Bot.* **10** 290-301
- [22] Sakanoue S 2007 *Ecol. Modelling* **205** 159-168
- [23] Goel N S, Maitra S C and Montroll E W 1971 *Rev. Mod. Phys.* **43** 231
- [24] Román P R and Ruiz F T 2012 *Biosys.* **110** 9-21

- [25] Tjørve K M C and Tjørve E 2017 *Plos One* **12** e0178691
- [26] Sen P N 2003 *Chem. Phys.* **119** 9871
- [27] Wu J and Berland K M 2008 *Biophys. J.* **95** 2049-2052
- [28] Rubchinsky L and Sushchik M 1999 *Internat. J. Bifur. Chaos* **9** 2329-2333
- [29] Bragard J, Boccaletti S and F. T. Arecchi F T 2001 *Internat. J. Bifur. Chaos* **11** 2715-2729
- [30] Russo G and Slotine J J E 2011 *Phys. Rev. E* **84** 041929
- [31] Nicolaou Z G, Case D J, van der Wee E B, Driscoll M M and Motter A R 2021 *Nature Commun.* **12** 4486
- [32] Wang Y, Wang X, Ren D, Ma Y and Wang C 2021 *Phys. Rev. E* **103** 032414
- [33] Pikovsky A S, Rosenblum M G and Kurths J 2001 *Synchronization: A Universal Concept in Nonlinear Sciences* (Cambridge: Cambridge University Press)
- [34] Boccaletti S, Kurths J, Osipov G, Valladares D L and Zhou C S 2002 *Phys. Rep.* **366** 1-101
- [35] Mosekilde E, Maistrenko Y and Postnov D 2002 *Chaotic Synchronization: Applications to Living Systems* (Singapore: World Scientific)
- [36] Strogatz S H 2004 *Sync: How Order Emerges From Chaos in The Universe, Nature, and Daily Life* (New York: Hyperion)
- [37] Barabás G, Parent C, Kraemer A, de Perre F V and De Laender F 2022 *Nat. Commun.* **13** 2521
- [38] Manchein C, da Silva R M and Beims M W 2017 *Chaos* **27** (2017) 081101.
- [39] da Silva R M, Manchein C and Beims M W 2017 *Chaos* **27** 103101.
- [40] Dudkowski D, Jafari S, Kapitaniak T, Kuznetsov N V, Leonov G A and Prasad A 2016 *Phys. Rep.* **637** 1-50
- [41] Zaslavsky G M 2002 *Physica D* **168** 292-304
- [42] Manrubia S C, Mikhailov A S and Zanette D H 2004 *Emergence of Dynamical Order* (Singapore: World Scientific)
- [43] Yam Y B 2019 *Dynamics of Complex Systems* (New York: Routledge)
- [44] Arnonld L 2002 *Random Dynamical Systems* (Berlin: Springer-Verlag)
- [45] Freidlin M I and Wentzell A D 2012 *Random Perturbations of Dynamical Systems* (Berlin: Springer)
- [46] Filho J V S, Raposo E P, Macedo A M S, Vasconcelos G L, Viswanathan G M, Bartumeus F and da Luz M G E 2020 *J. Stat. Mec. The. Exp.* **2** 023406

- [47] Risken H 1996 *The Fokker-Planck Equation*, second ed. (Berlin: Springer-Verlag)
- [48] Gardiner C W 1997 *Handbook of Stochastic Methods* (Berlin: Springer-Verlag)
- [49] Coffey W T and Kalmykov Y P 2017 *The Langevin equation: With applications to stochastic problems in physics, chemistry, and electrical engineering* (New Jersey: World Scientific)
- [50] Gitterman M 2005 *The Noisy Oscillator* (Singapore: World Scientific)
- [51] Snook I 2007 *The Langevin and Generalised Langevin Approach to the Dynamics of Atomic, Polymeric and Colloidal Systems* (Amsterdam: Elsevier)
- [52] Fa K S 2018 *Langevin and Fokker-Planck equations and their generalizations* (Singapore: World Scientific)
- [53] Nadtochy P N, Schmitt C and Mazurek K 2013 *Phys. Scr.* **2013** 014004
- [54] Li D-Z, Zeng J-R, Huang W-J, Yao Y and Yang X-B 2023 *Phys. Scr.* **98** 025218
- [55] Stanislavsky A A 2003 *Phys. Scr.* **67** 265
- [56] Yang Q, Liu F and Turner I 2009 *Phys. Scr.* **2009** 014026
- [57] Fernández F M 2009 *Phys. Scr.* **80** 065010
- [58] Jafari M A and Aminataei A 2009 *Phys. Scr.* **80** 055001
- [59] Zoppou C and Knight J H 1999 *App. Math. Modelling* **23** 667-685
- [60] Ahmad Z 2000 *ISH J. Hydraulic Eng.* **6** 46-54
- [61] Rais D, Mensik M, Paruzel B, Toman P and Pflieger J 2018 *J. Phys. Chem. C* **122** 22876
- [62] Tilahun M and Yergou B Tatek Y B 2023 *Phys. Scr.* **98** 025006
- [63] Dudko O K, Berezhkovskii A M and Weiss G H 2005 *J. Phys. Chem. B* **109** 21296-21299
- [64] Richardson L F 1926 *Proc. R. Soc. Lond. A* **110** 709-737
- [65] Komolgorov A N 1941 *Dokl. Acad. Sci. URSS* **30** 301-305
- [66] Batchelor G K 1952 *Proc. Cambridge Philos. Soc.* **48** 345-362
- [67] Okubo A 1962 *J. Oceanogr. Soc. Jpn.* **20** 286-320
- [68] Hentschel H G E and Procaccia I 1984 *Phys. Rev. A* **29** 1461
- [69] Fa K S 2005 *Phys. Rev. E* **72** 020101
- [70] Fa K S 2021 *Phys. Scr.* **96** 055002
- [71] Fa K S 2021 *J. Stat. Mech.* **9** 093205
- [72] Fa K S 2011 *Phys. Rev. E* **84** 012102
- [73] Schimansky-Geier L and Zülicke C 1990 *Z. Phys. B* **79** 451
- [74] Barzykin A V and Seki K 1997 *Europhys. Lett.* **40** 117

- [75] Wang K G and Tokuyama M 1999 *Physica A* **265** 341-351
- [76] Calisto H and Bologna M 2007 *Phys. Rev. E* **75** 050103
- [77] Jiménez-Aquino J I and Romero-Bastida M 2012 *Phys. Rev. E* **86** 061115
- [78] Yu T, Zhang L and Luo MK 2013 *Phys. Scr.* **88** 045008
- [79] Fa K S 2016 *Eur. J. Phys.* **37** 065101
- [80] Fa K S 2019 *J. Stat. Mech.* **6** 063205
- [81] Fa K S 2020 *Phys. Scr.* **95** 025004
- [82] Fa K S 2020 *Physica A* **545** 123334
- [83] Bonatti C 2006, Generic Properties of Dynamical Systems in *Encyclopedia of Mathematical Physics* Françoise J P, Naber G L, Tsun T S (Eds.), pp 494-502 (Cambgridge: Academic Press)
- [84] Afraimovich V and Urias J 2003 *Commun. Nonlinear Sci. Numer. Simul.* **8** 171-181
- [85] Fa K S 2020 *J. Stat. Mech.* **9** 093206
- [86] Bluman G W and Cole J D 1974 *Similarity Methods for Differential Equations* (Berlin: Springer-Verlag)
- [87] Lin W L and Ho C L 2012 *Ann. Phys.* **327** 386-397
- [88] Ho C L 2013 *J. Math. Phys.* **54** 041501
- [89] Ho C L and Sasaki R 2014 *J. Math. Phys.* **55** 113301
- [90] Ho C L and Yang C M 2019 *Chin. J. Phys.* **59** 1117-125
- [91] Llibre J, Ramírez R and Ramírez V 2023 *Dynamics through First-Order Differential Equations in the Configuration Space* (Berlin: Birkhäuser)
- [92] Raducha T and Miguel M S 2020 *Sci. Rep.* **10** 15660
- [93] Bellavia S, Guriolli G, Morini B and Toint P L 2023 *J. Optim. Theory Appl.* **196** 700
- [94] Lindner B, G-Ojalvo J, Neiman A and S-Geier L 2004 *Phys. Rep.* **392** 321
- [95] E. Agazzi, L. Montecucco (Eds.) 2002 *Complexity and Emergence* (Singapore: World Scientific)
- [96] Albeverio S, Mastrogiacomo E, Gianin E R and Ugolini S (Eds.) 2022 *Complexity and Emergence* (Cham: Springer)
- [97] Avalos J B and Pagonabarraga I 1995 *Phys. Rev. E* **52** 5881.
- [98] Ryabov A, Holubec V and Berestneva E 2019 *J. Stat. Mec. Theor. Exp.* **8** 084014.
- [99] Mazumdar E, Westenbroek T, Jordan M I and Sastry S S 2020 *59th IEEE Conference on*

Decision and Control (CDC) 4275-4280

[100] Callaham J L, Loiseau J C, Rigas G and Brunton L S 2021 *Proc. R. Soc. A* **477** 20210092.

[101] Zhao K 2022 *Fractal Fract.* **6** 725.